

Supplementary Figures

TGF- β -dependent reprogramming of amino acid metabolism induces epithelial–mesenchymal transition in non-small cell lung cancers

Fumie Nakasuka^{1,2,3,4,16}, Sho Tabata^{1,2,5,6,16,17*}, Takeharu Sakamoto^{7,8}, Akiyoshi Hirayama^{1,2}, Hiromichi Ebi⁹, Tadaaki Yamada¹⁰, Ko Umetsu¹, Maki Ohishi¹, Ayano Ueno¹, Hisatsugu Goto¹¹, Masahiro Sugimoto^{1,2,12}, Yasuhiko Nishioka¹¹, Yasuhiro Yamada^{3,4}, Masaru Tomita^{1,2}, Atsuo T. Sasaki^{1,5,13,14}, Seiji Yano¹⁵, and Tomoyoshi Soga^{1,2}

¹Institute for Advanced Biosciences, Keio University, Tsuruoka, Yamagata 997-0052, Japan

²Systems Biology Program, Graduate School of Media and Governance, Keio University, Fujisawa, Kanagawa 252-0882, Japan

³Department of Computational Biology and Medical Sciences, Graduate School of Frontier Sciences, The University of Tokyo, Chiba 277-8561, Japan

⁴Division of Stem Cell Pathology, Center for Experimental Medicine and Systems Biology, Institute of Medical Science, The University of Tokyo, Tokyo 108-8639, Japan

⁵Division of Hematology and Oncology, Department of Internal Medicine, University of Cincinnati, Cincinnati, OH 45267, USA.

⁶Institute for Protein Research, Osaka University, Suita, Osaka 565-0871, Japan

⁷Division of Cellular and Molecular Biology, The Institute of Medical Science, The University of Tokyo, Minato-ku, Tokyo 108-8639, Japan

⁸Department of System Biology, Institute of Medical, Pharmaceutical and Health Sciences, Kanazawa University, Takaramachi, Kanazawa, Ishikawa 920-8640, Japan

⁹Division of Molecular Therapeutics, Aichi Cancer Center Research Institute, Nagoya, Aichi 464-8681, Japan.

¹⁰Department of Pulmonary Medicine, Kyoto Prefectural University of Medicine, Kamigyo-ku, Kyoto 602–8566, Japan

¹¹Department of Respiratory Medicine and Rheumatology, Graduate School of Biomedical Sciences, Tokushima University, Tokushima, Tokushima 770-8503, Japan

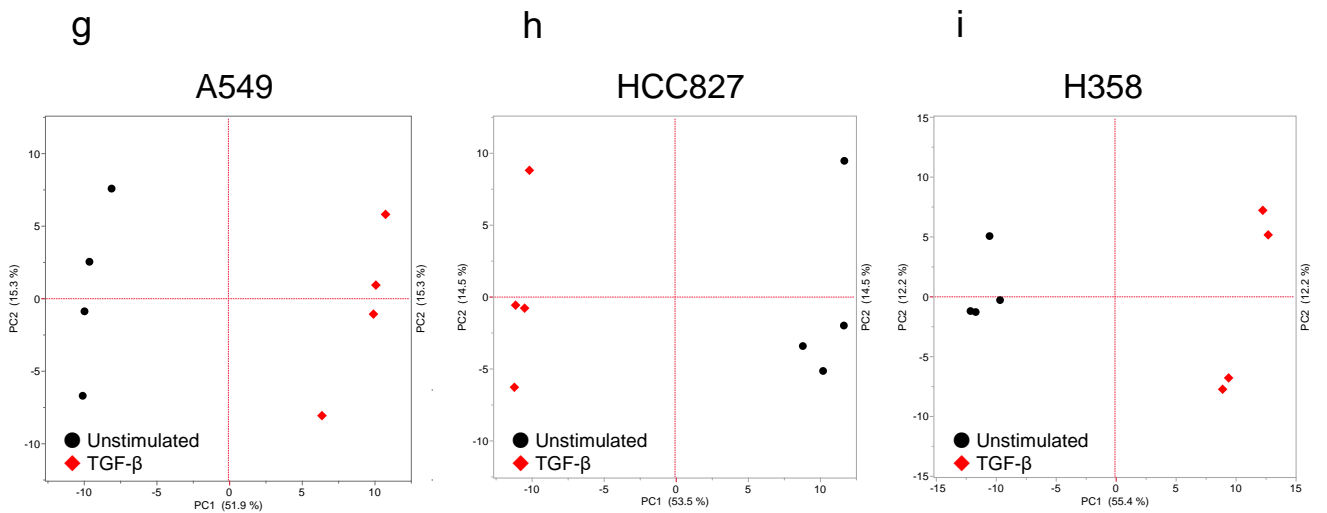
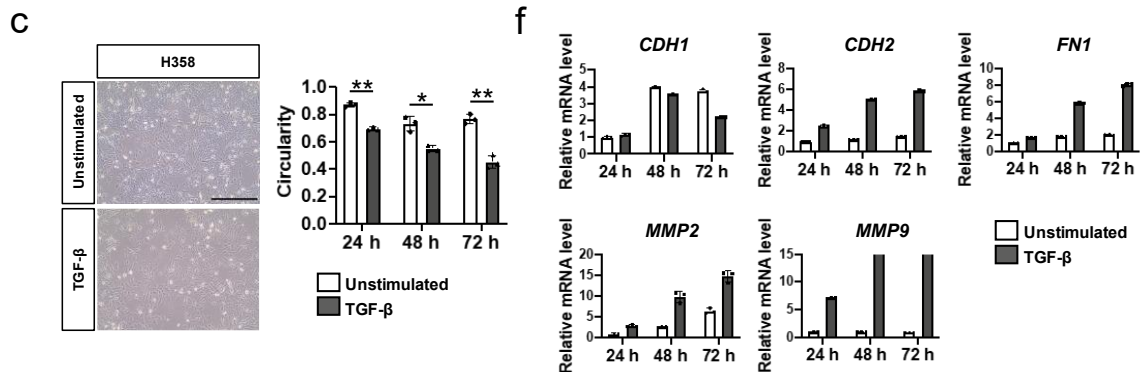
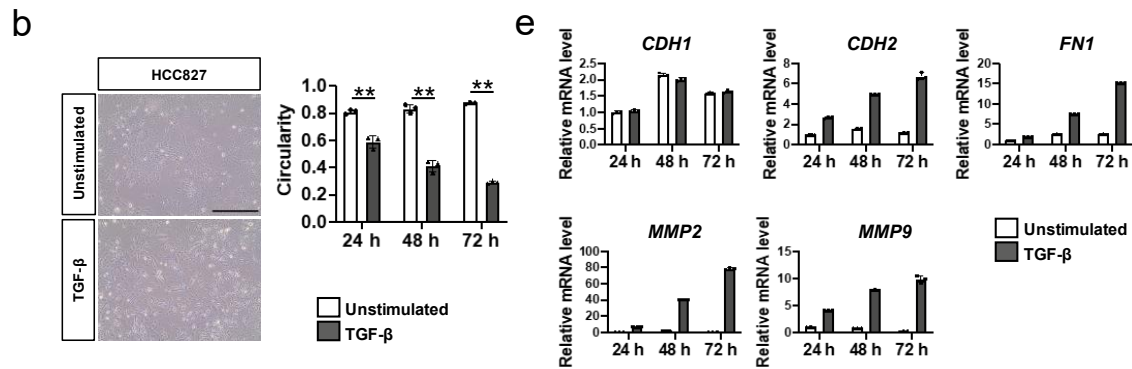
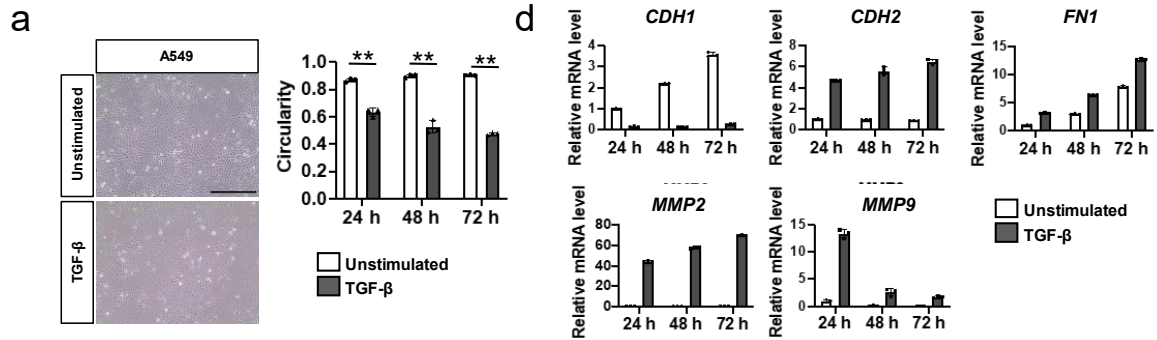
¹²Health Promotion and Preemptive Medicine, Research and Development Center for Minimally Invasive Therapies, Tokyo Medical University, Shinjuku, Tokyo 160-0022, Japan

¹³Department of Cancer Biology, University of Cincinnati College of Medicine, OH 45267, USA

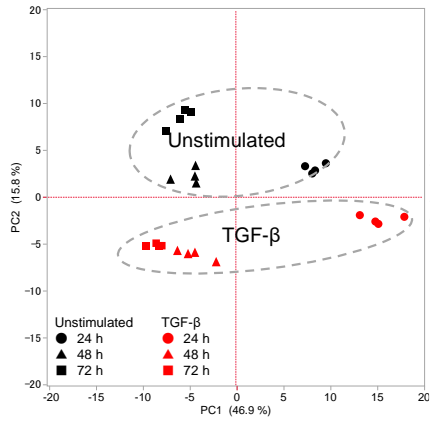
¹⁴Department of Neurosurgery, Brain Tumor Center at UC Gardner Neuroscience Institute, Cincinnati, OH 45267, USA

¹⁵Department of Medical Oncology, Kanazawa University Cancer Research Institute, Kanazawa University, Kanazawa, Ishikawa 920-0934, Japan

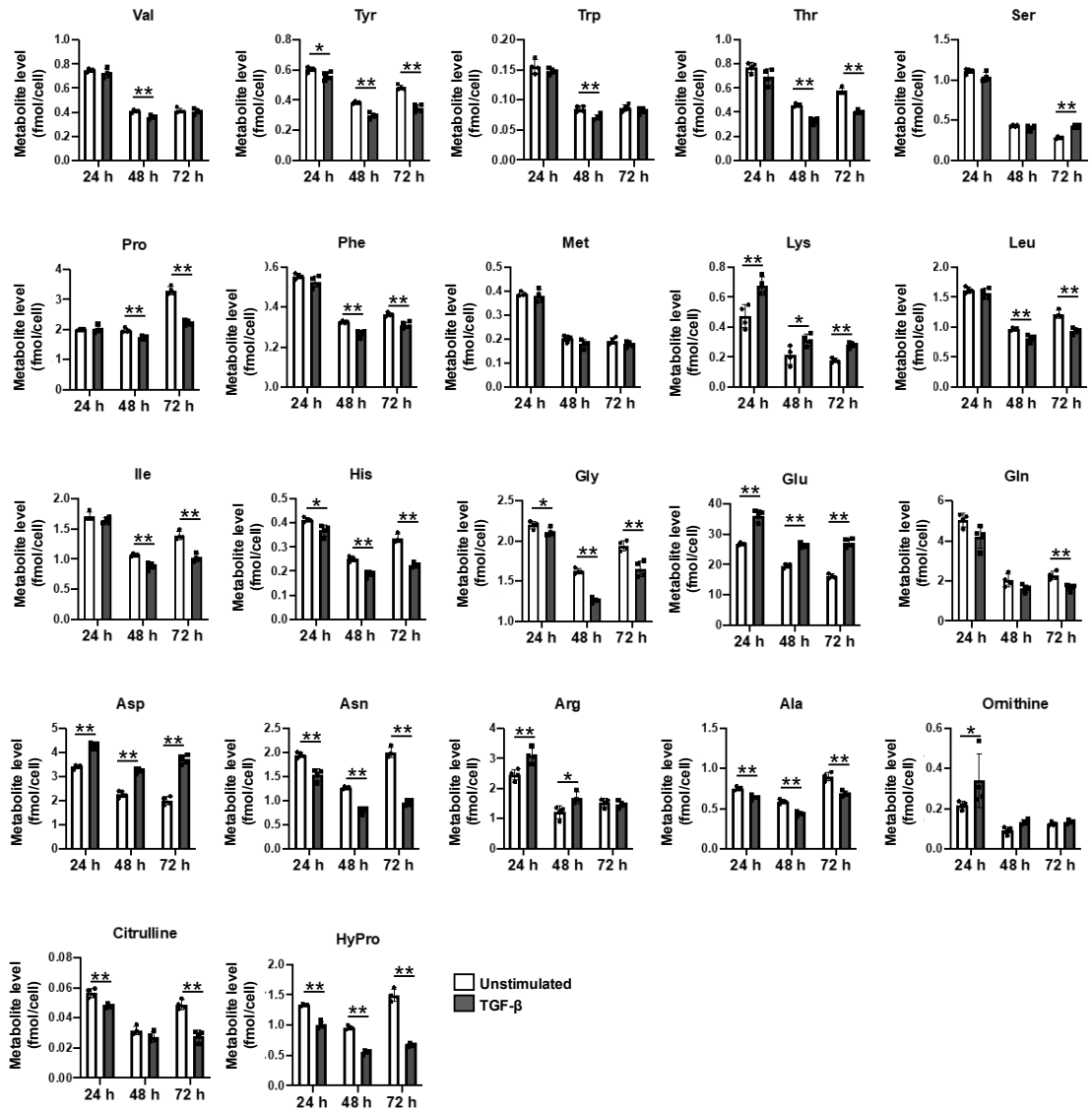
¹⁶These authors contributed equally to this work



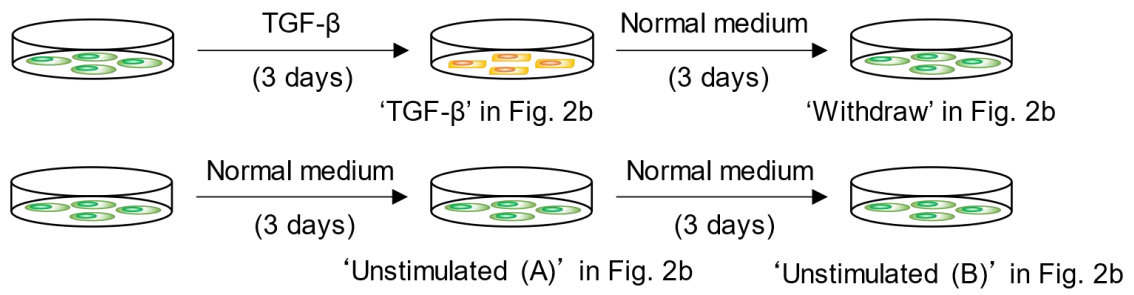
j



k

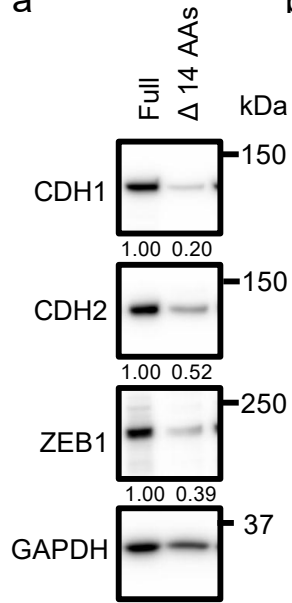


Supplementary Fig. 1 Related to Figure 1. (a–c) Morphological changes in TGF- β -stimulated (a) A549, (b) HCC827, and (c) H358 cells. Cells were seeded at a density of 2.0×10^5 cells/well in a 6-well plate and stimulated with 5 ng/mL TGF- β for 24, 48, and 72 h. Cells were observed by phase contrast inverted microscope at 100 \times magnification. Scale bar, 500 μ m. Cell morphology was determined by calculating cell circularity using ImageJ software. (d–f) Expression of epithelial–mesenchymal transition (EMT) marker genes in (d) A549, (e) HCC827, and (f) H358 cells stimulated with or without 5 ng/mL TGF- β . mRNA expression levels of *CDH1*, *CDH2*, *FNI*, *MMP2*, and *MMP9* were measured using real-time PCR. (g–i) Score plots of principal component analysis (PCA) for metabolomics profiles of (g) A549, (h) HCC827, and (i) H358 cells stimulated with or without TGF- β (n = 4). Cells were cultured in the presence of 2 ng/mL TGF- β for 2–5 weeks to induce EMT. Metabolite levels were detected by capillary electrophoresis time-of-flight mass spectrometry (CE-TOFMS). The black and red plots indicate unstimulated and TGF- β -stimulated cells, respectively. (j) PCA for metabolomics profiles of A549 cells stimulated with 5 ng/mL TGF- β for 24, 48, and 72 h (n = 4). The black and red plots indicate unstimulated and TGF- β -stimulated cells, respectively. (k) Intracellular free-amino acids levels in A549 cells stimulated with TGF- β for 24, 48, and 72 h. The concentrations (fmol/cell) of each amino acid (n = 4). **P* < 0.05, ***P* < 0.01.

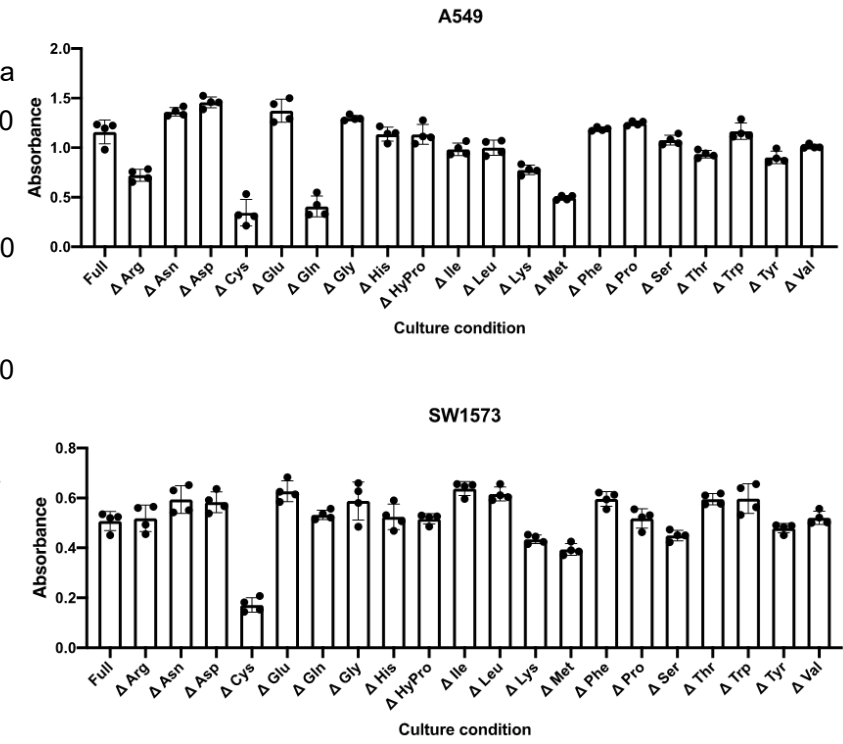


Supplementary Fig. 2 Related to Figure 2. Schematic diagram of sample preparation in Fig. 2b.

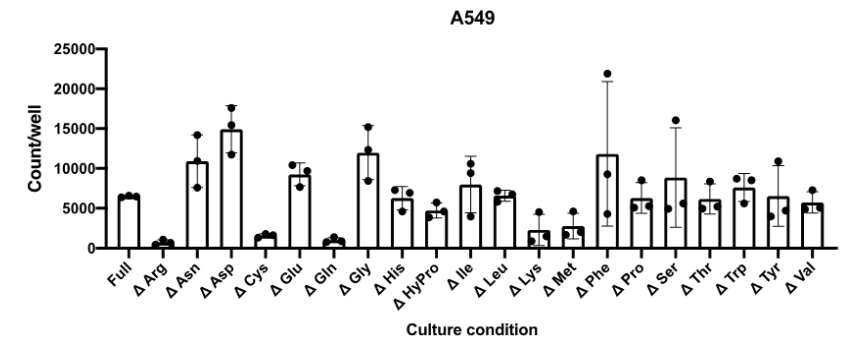
a

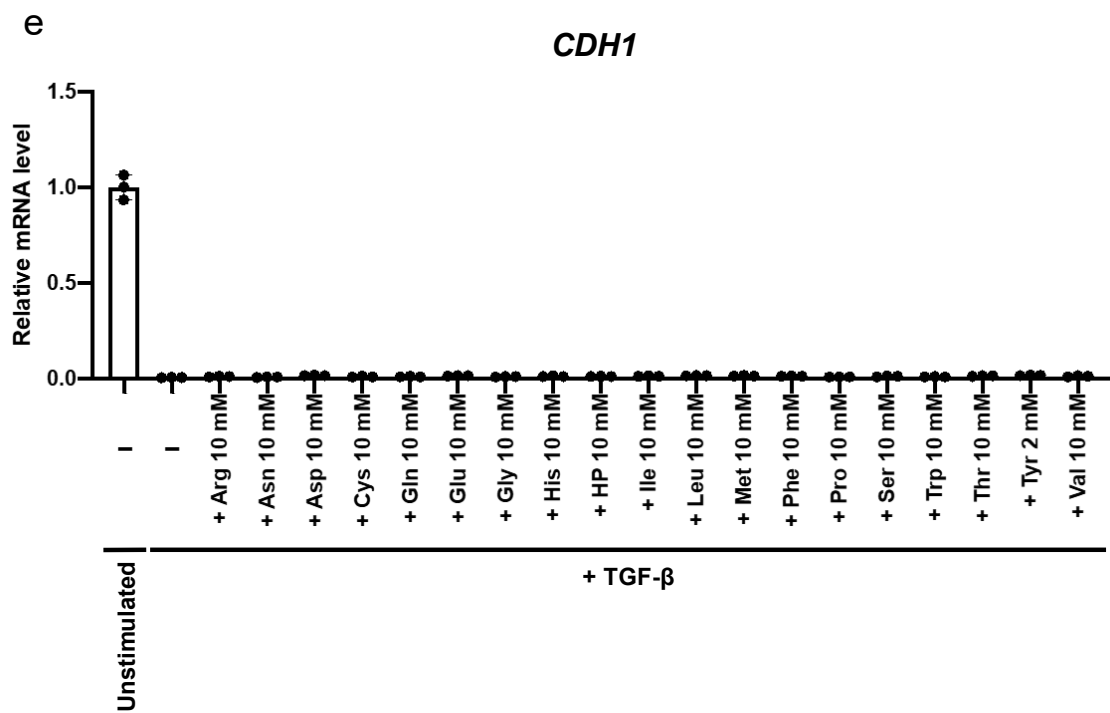
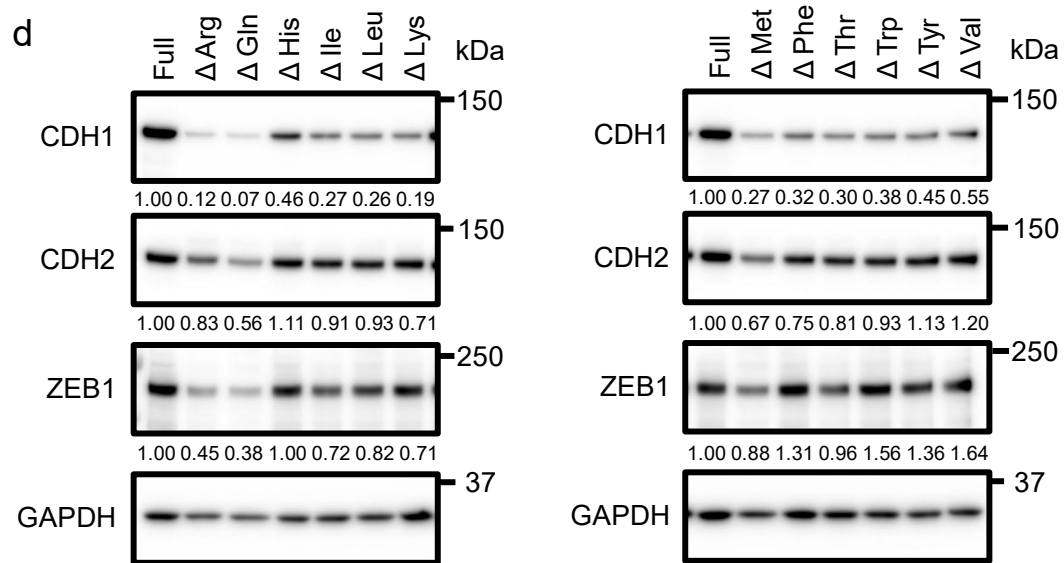


b

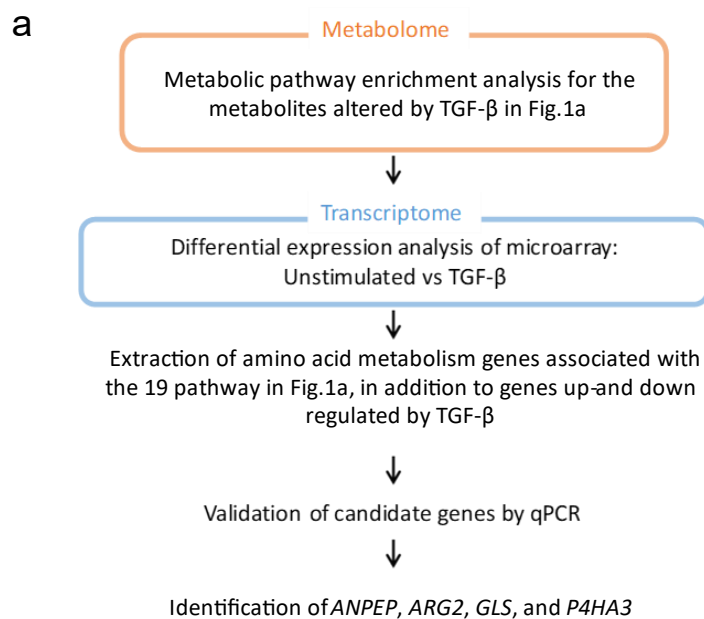


c





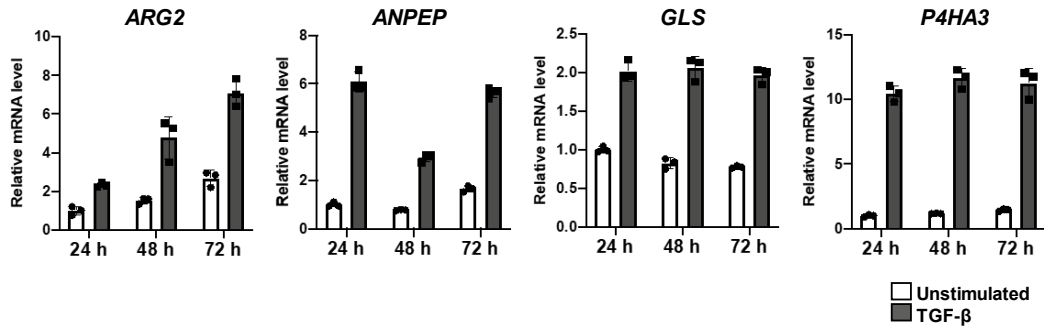
Supplementary Fig. 3 Related to Figure 3. (a) Effect of the combined deletion of Met, Val, Pro, Trp, Leu, Ile, Phe, Gly, Tyr, His, Ala, Thr, Asn, and hydroxyproline on the expression of EMT markers. CDH1, CDH2 and ZEB1 protein abundance quantified by western blotting using Image J software. Each protein is normalized to GAPDH levels and are presented as fold-change relative to those under regular conditions with full amino acids. (b) Effects of amino acid deprivation on cell viability in A549 and SW1573 cells assessed using MTT assay. (c) Effects of amino acid deprivation on cell viability in A549 cells assessed using DAPI staining. (d) Effects of amino acid depletion on CDH1, CDH2 and ZEB1 protein expression in A549 cells. (e) Effects of amino acid addition on mRNA expression of epithelial marker gene *CDH1* in A549 cells. Cells were treated with 5 ng/mL TGF- β and the indicated amino acid concentration for 72 h. mRNA expression levels were measured using real-time PCR. Data are presented as mean \pm SD.



b

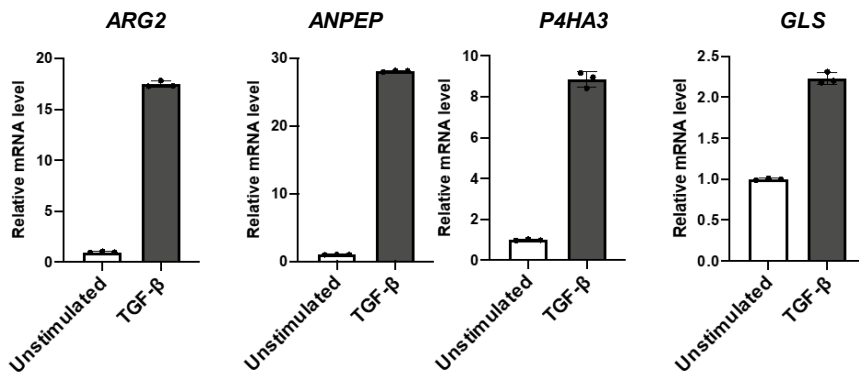
Metabolic pathways	Metabolism-related genes (F.C.)
Histidine-glutamate-glutamine metabolism	<i>GLS</i> (3.47)
Histidine-glutamate-glutamine and proline metabolism/ Rodent version	<i>P4HA3</i> (9.01) , <i>GLS</i> (3.47)
Nociception_Pro-nociceptive action of Nociceptin in spinal cord at low doses	-
Glycine, serine, cysteine and threonine metabolism	-
Methionine-cysteine-glutamate metabolism	<i>DNMT3B</i> (2.66)
Aspartate and asparagine metabolism	-
Neurophysiological process_GABAergic neurotransmission	-
L-Alanine, L-Cysteine, and L-Methionine metabolism / Human version	-
Urea cycle	<i>ARG2</i> (3.81)
Neurophysiological process_Circadian rhythm	<i>GLS</i> (3.47)
Nitrogen metabolism	<i>GLS</i> (3.47)
Propionate metabolism p.2	<i>OXCT1</i> (4.19)
Glutathione metabolism / Rodent version	<i>ANPEP</i> (3.99)
Regulation of lipid metabolism_PPAR regulation of lipid metabolism	-
Taurine and hypotaurine metabolism	-
Gamma-aminobutyrate (GABA) biosynthesis and metabolism	-
Arginine metabolism/ Rodent version	<i>ARG2</i> (3.81)
CTP/UTP metabolism	<i>DPYD</i> (2.22) , <i>CTPS</i> (3.13)
(L)-Arginine metabolism	<i>ARG2</i> (3.81)
Glycine links	-
Acetyl-CoA links	-

C

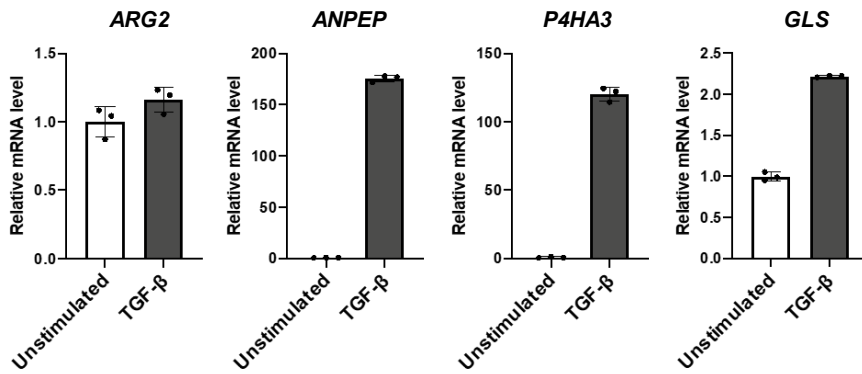


d

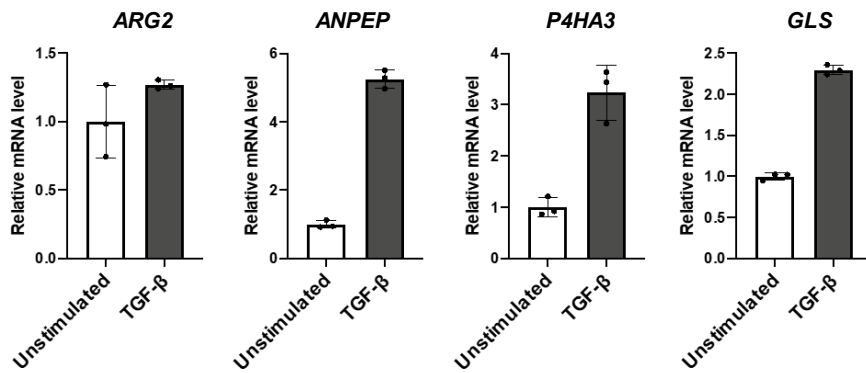
A549



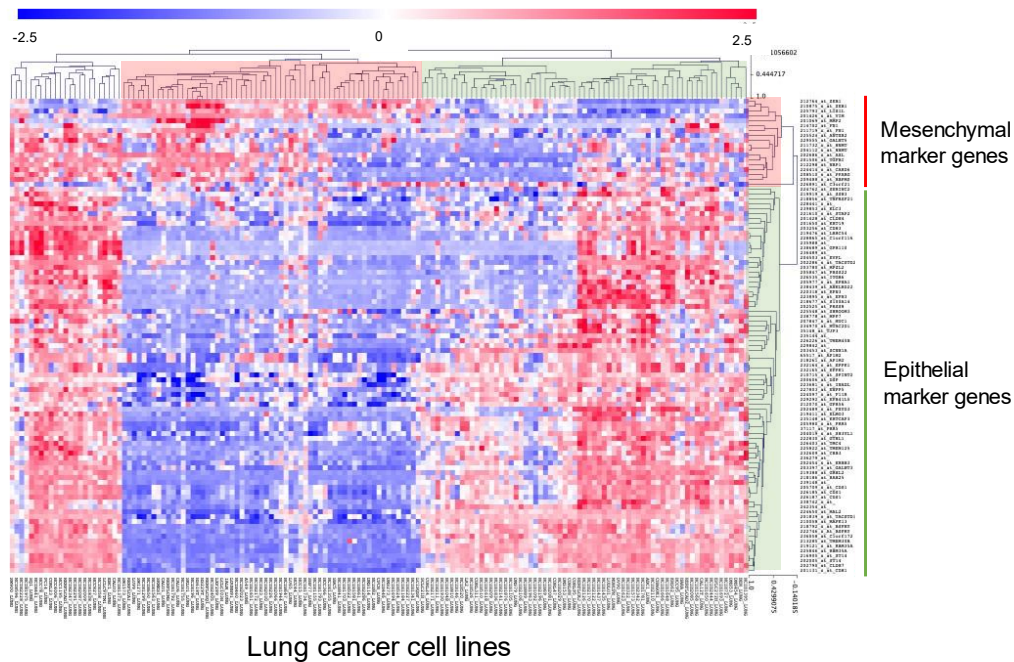
HCC827



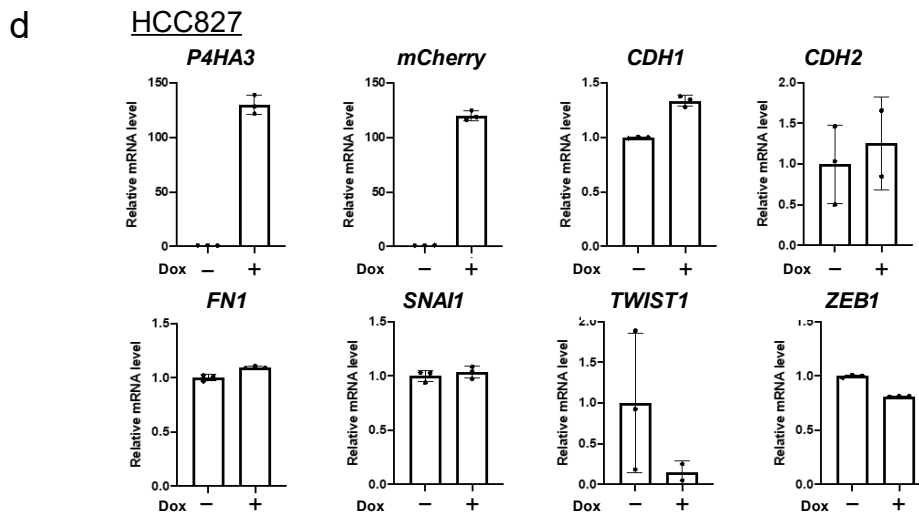
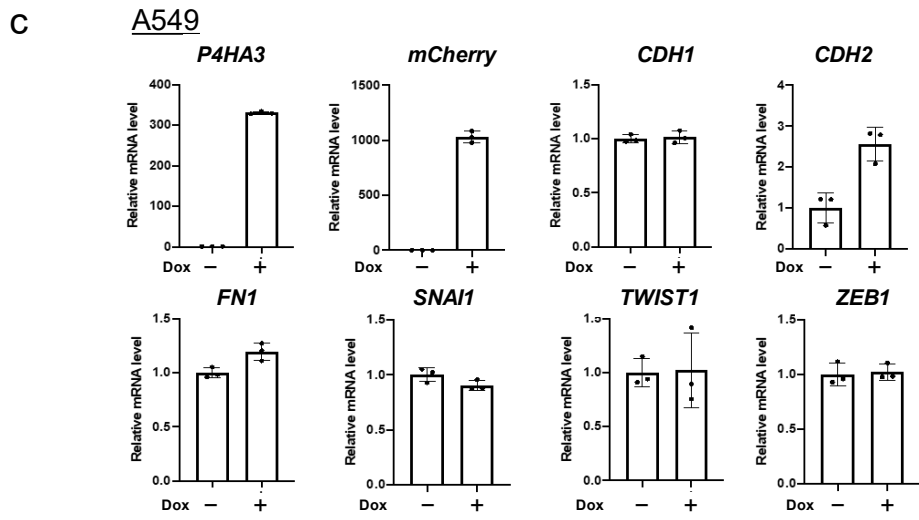
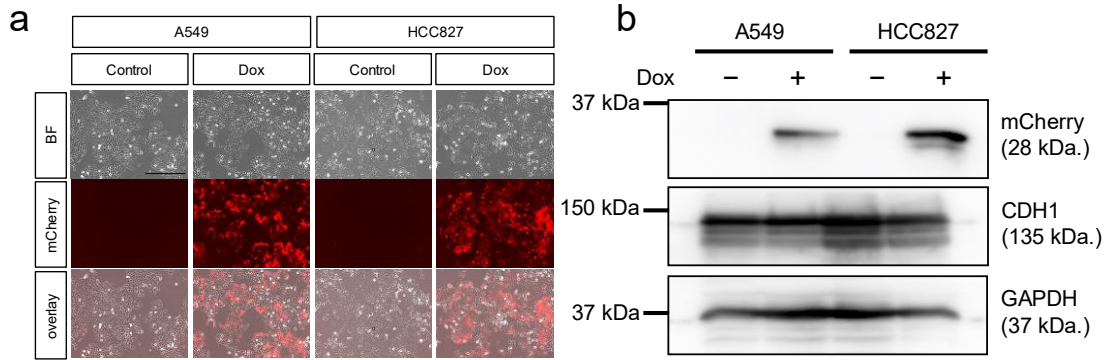
H358



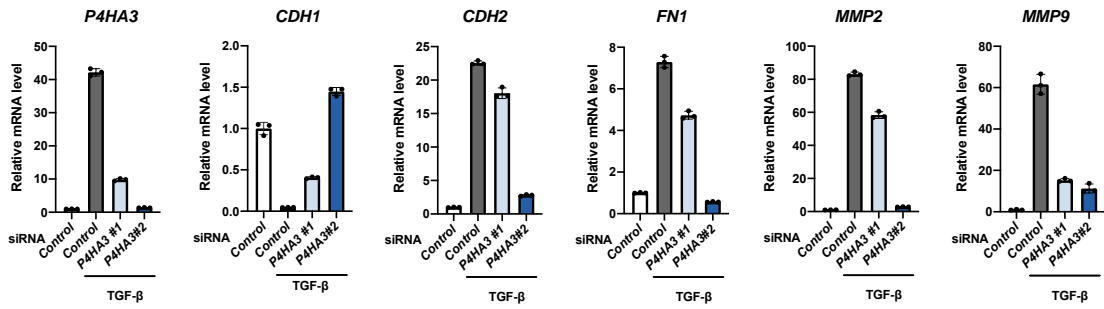
e



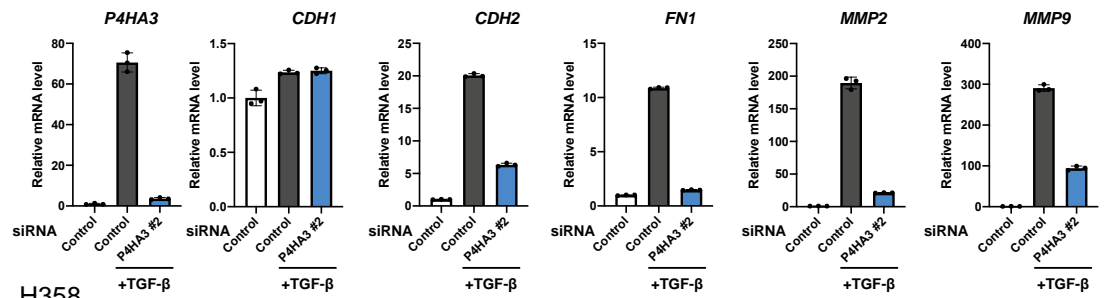
Supplementary Fig. 4 Related to Figure 4. (a) Scheme of data processing for identification of epithelial–mesenchymal transition (EMT)-related amino acid metabolism genes using datasets of metabolome and transcriptome. (b) List of 21 metabolic pathways mentioned in Fig. 1a and metabolism-related genes that were up- or down-regulated by TGF- β . mRNA levels of metabolism-related genes were measured by a microarray. (c) Expression of *ANPEP*, *ARG2*, *GLS*, and *P4HA3* in A549 cells stimulated with or without 5 ng/mL TGF- β for 24, 48, and 72 h. (d) Expression of *ANPEP*, *ARG2*, *GLS*, and *P4HA3* in A549, HCC827, and H358 cells. Cells were cultured in the presence of 2 ng/mL TGF- β for 2–5 weeks to induce EMT. mRNA levels were measured by real-time PCR. (e) Cluster analysis of 76 EMT marker genes in lung cancer cell lines from Cancer Cell Line Encyclopedia dataset.



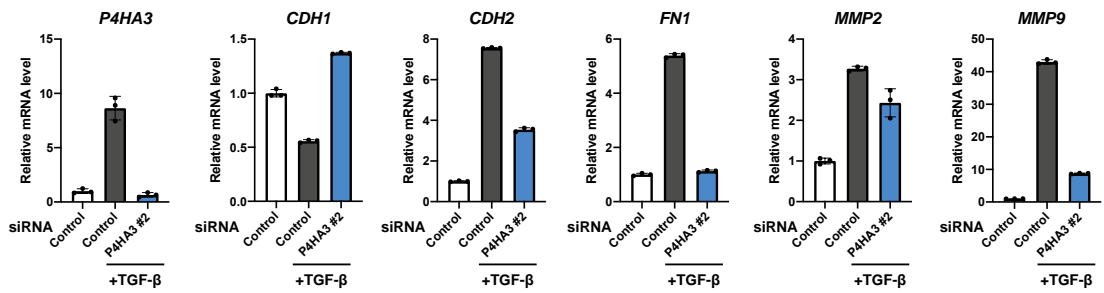
e A549



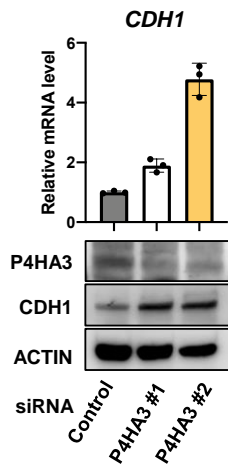
HCC827



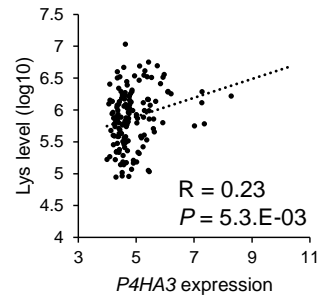
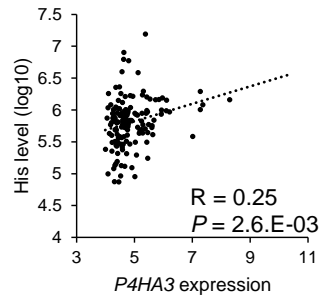
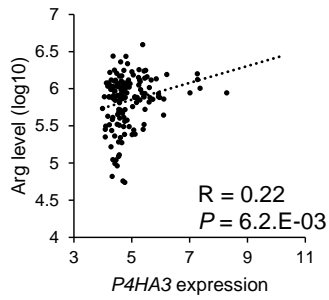
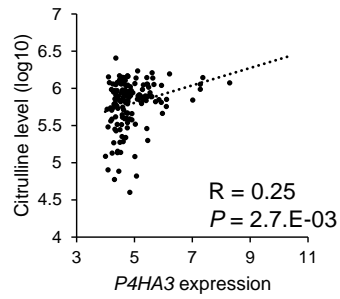
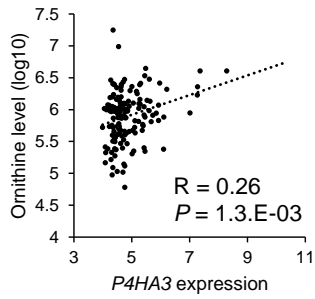
H358



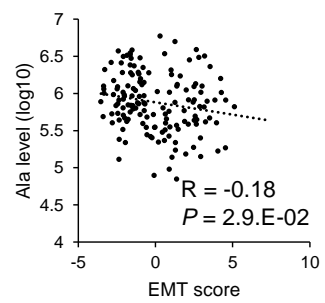
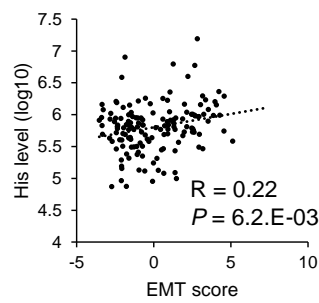
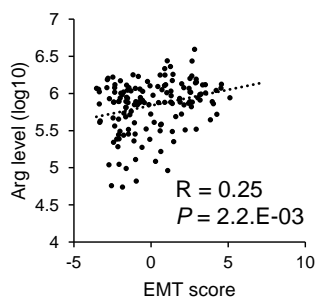
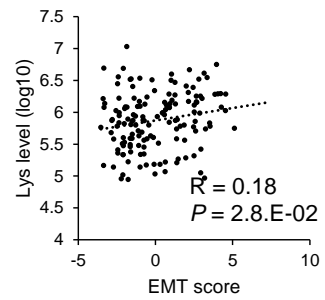
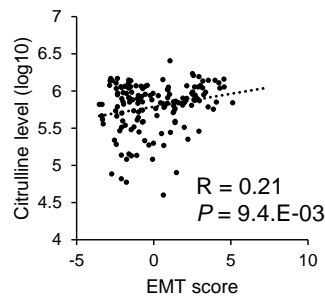
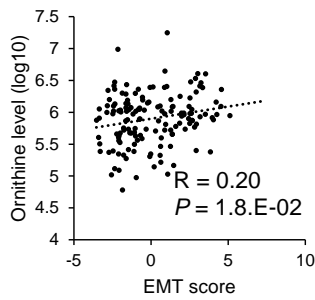
f



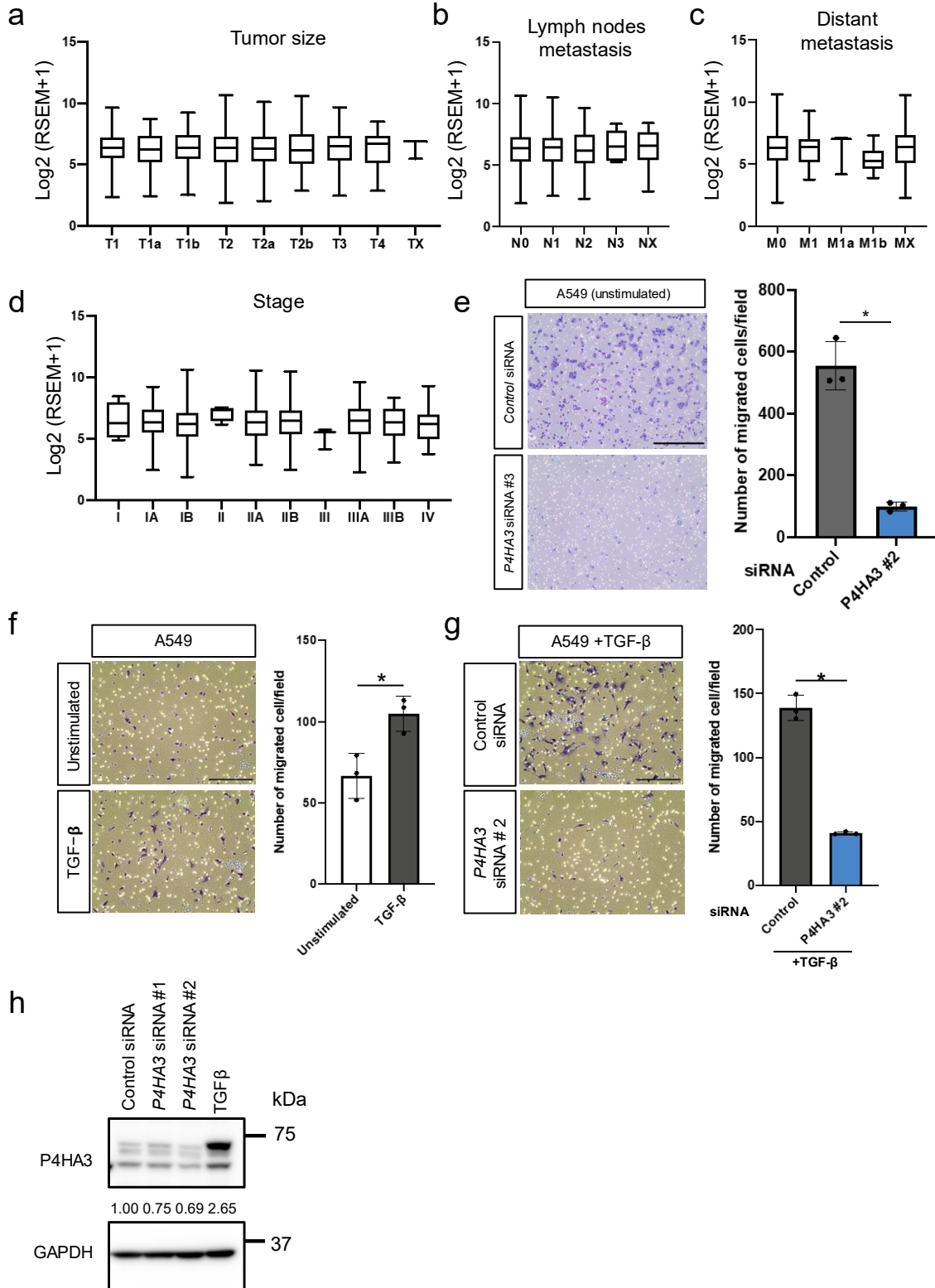
g P4HA3



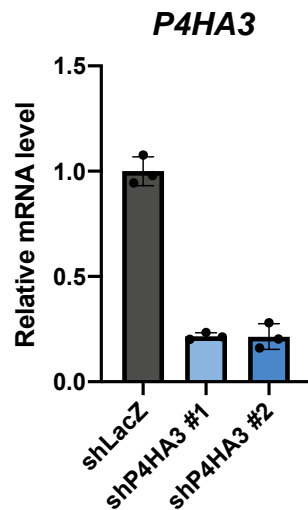
EMT score



Supplementary Fig. 5 Related to Figure 5. (a) Cell morphology and mCherry fluorescence in doxycycline (Dox) treated and untreated (Control) A549 and HCC827 cells observed by fluorescent microscope at 100× magnification. Scale bar, 500 μm. (b) Effect of P4HA3 overexpression on CDH1 protein levels in A549 and HCC827 cells as assessed by western blotting with GAPDH as the loading control. (c and d) Effect of P4HA3 overexpression on the expression of mRNA expression of various EMT markers in (c) A549 and (d) HCC827 cells measured by real-time PCR. Values are presented as mean ± SD from triplicate samples. (e) Effects of *P4HA3* siRNA on *EMT markers* and *P4HA3* mRNA expression in A549, HCC827, and H358 cells treated with TGF-β. (f) Effect of *P4HA3* siRNA on CDH1 levels in SW1573 cells. mRNA (upper) and protein (lower) levels of CDH1 were determined by real-time PCR and western blotting, respectively. Data for real-time PCR are presented as the mean ± SD. (g) Correlations between amino acids level, EMT score, and *P4HA3* mRNA expression in NSCLC cell lines from the CCLE dataset.



Supplementary Fig. 6 Related to Figure 6. (a–d) Box-and-whisker plot of *P4HA3* mRNA levels in (a) tumor size; T, (b) lymph node metastasis; N, (c) distant metastasis; M, and (d) stage. (e) Effect of *P4HA3* siRNA on migratory activity in A549 cells observed by bright field microscope at 100× magnification. Scale bar, 500 μm. Four random fields per sample were selected to enumerate the cells and each independent experiment was repeated in triplicate. Data are presented as migrated cells per field. **P* < 0.01. (f) Migratory activity of A549 cells treated with TGF-β. Scale bar, 250 μm. (g) Effects of *P4HA3* siRNA on migratory activity of A549 cells treated with TGF-β. Scale bar, 250 μm. (h) Knockdown efficiency of *P4HA3* siRNA in A549 cells. Protein levels in each sample were determined by western blotting. GAPDH was the loading control.



Supplementary Fig. 7 Related to Figure 7. Knockdown efficiency of *P4HA3* shRNA in A549 cells *in vitro*. mRNA levels in each sample were determined by real-time PCR. Values are presented as mean ± SD from triplicate samples.

Fig. 3b

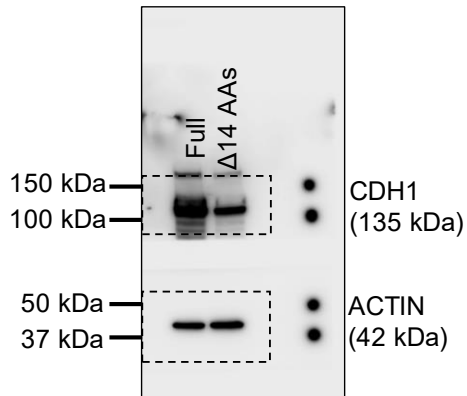


Fig. 3d: A549

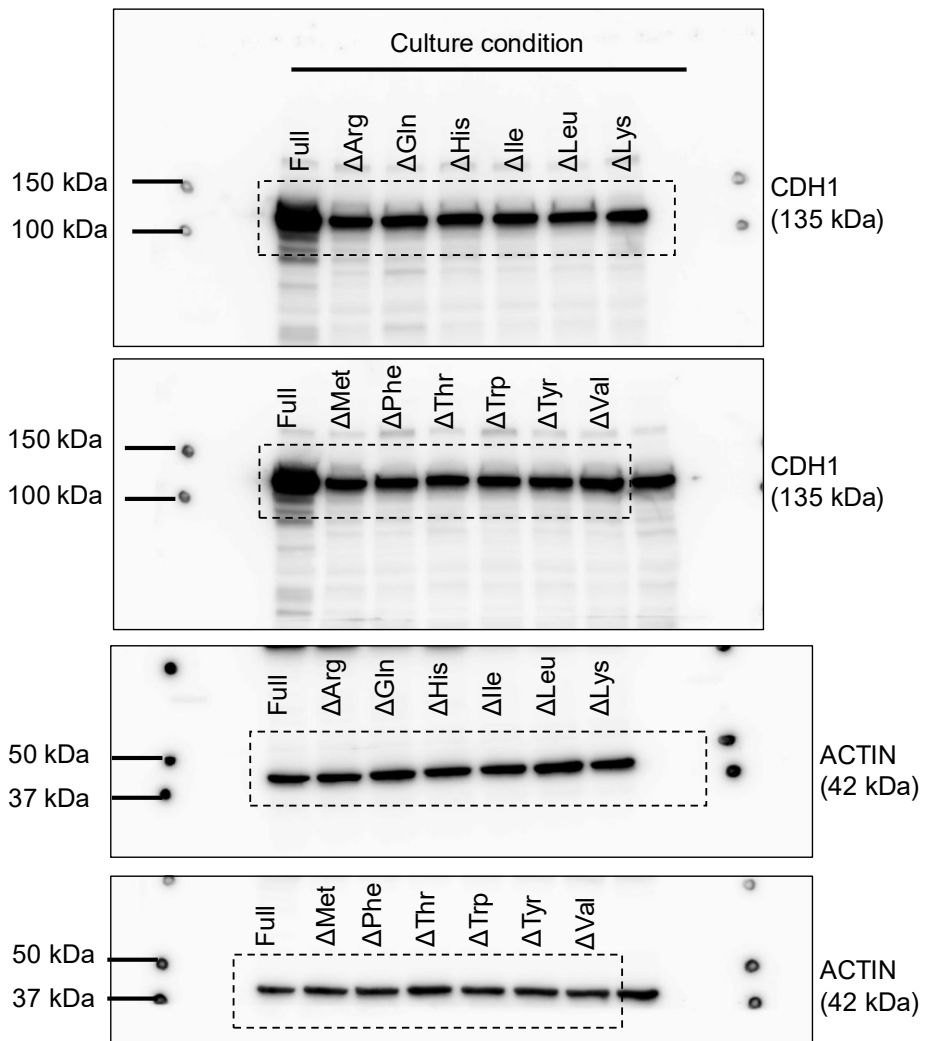
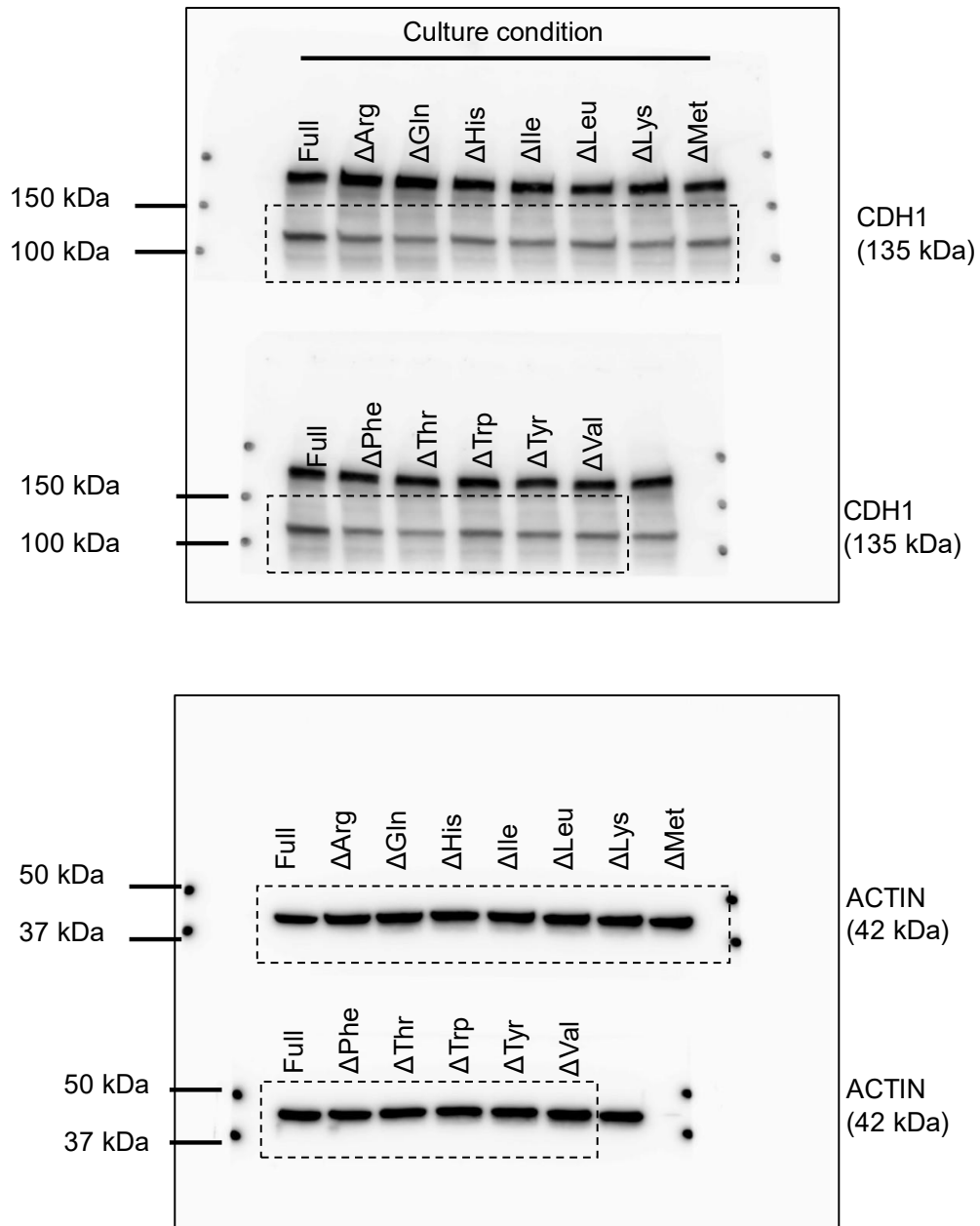
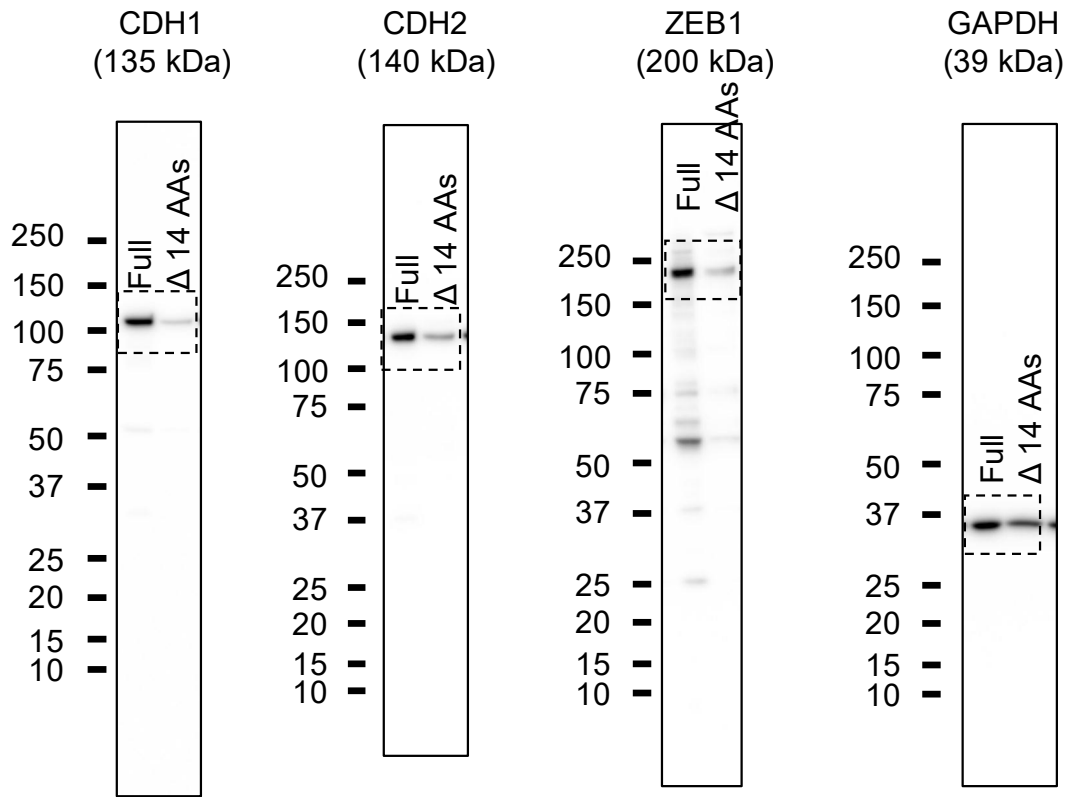


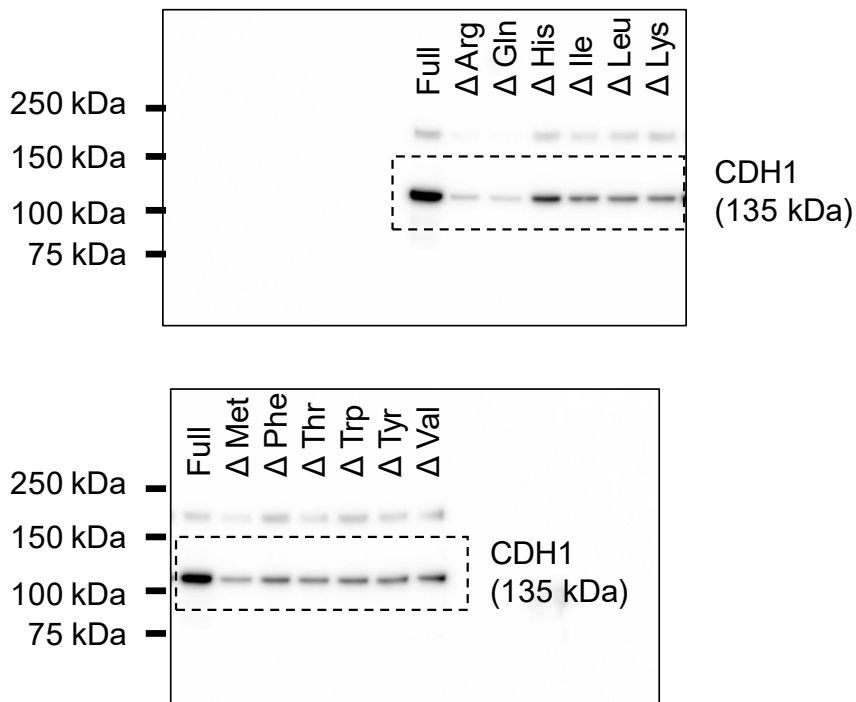
Fig. 3d: SW1573



Supplementary Fig. 3a



Supplementary Fig. 3d



Supplementary Fig. 3d

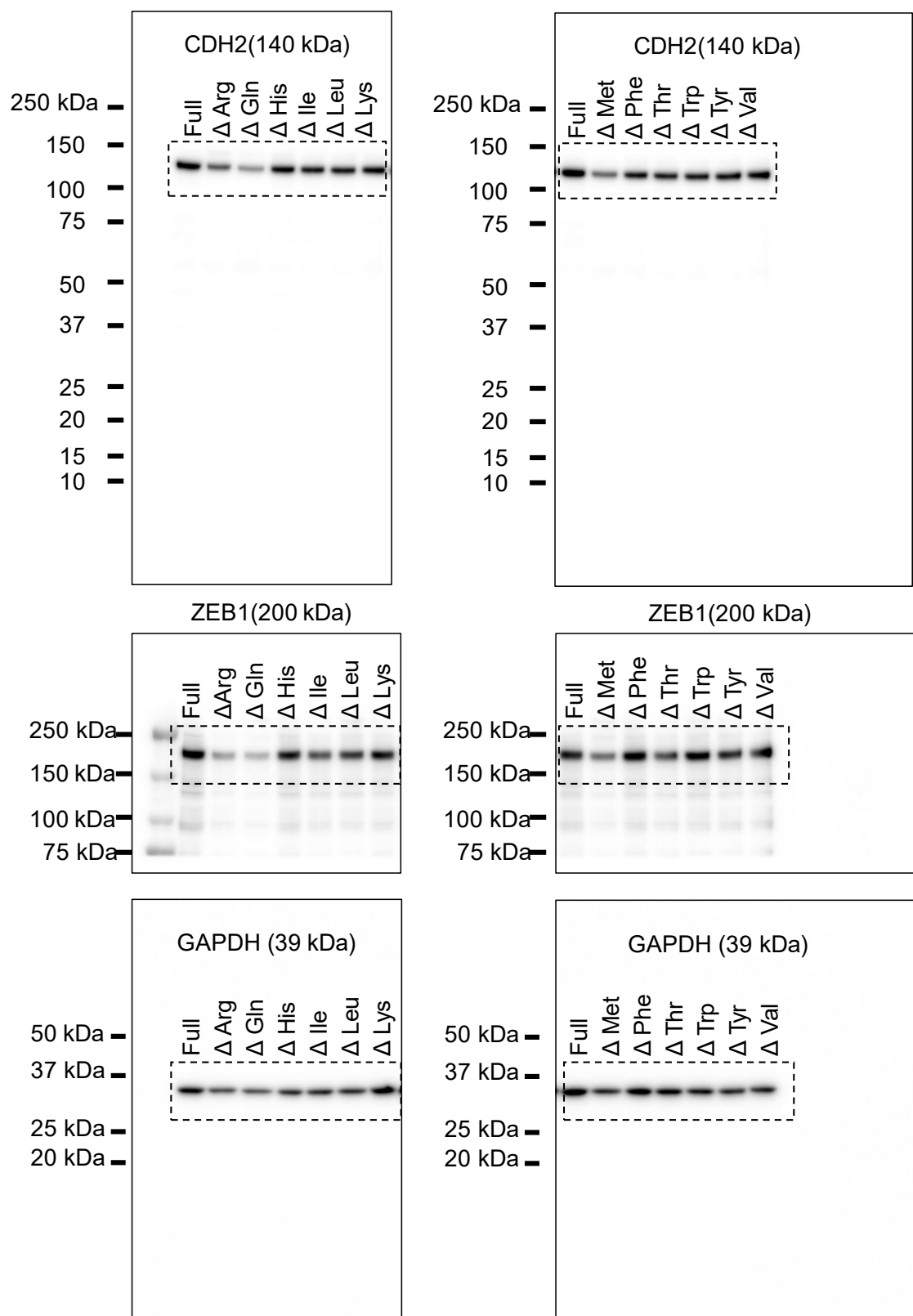
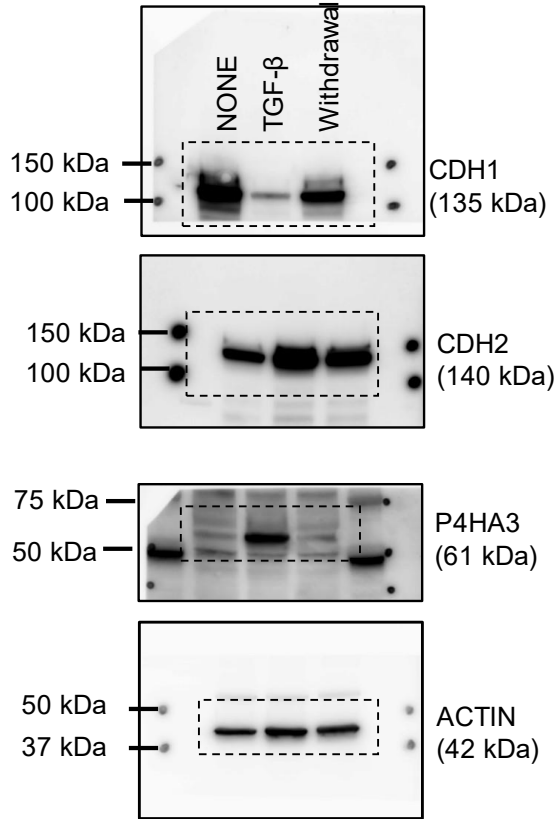
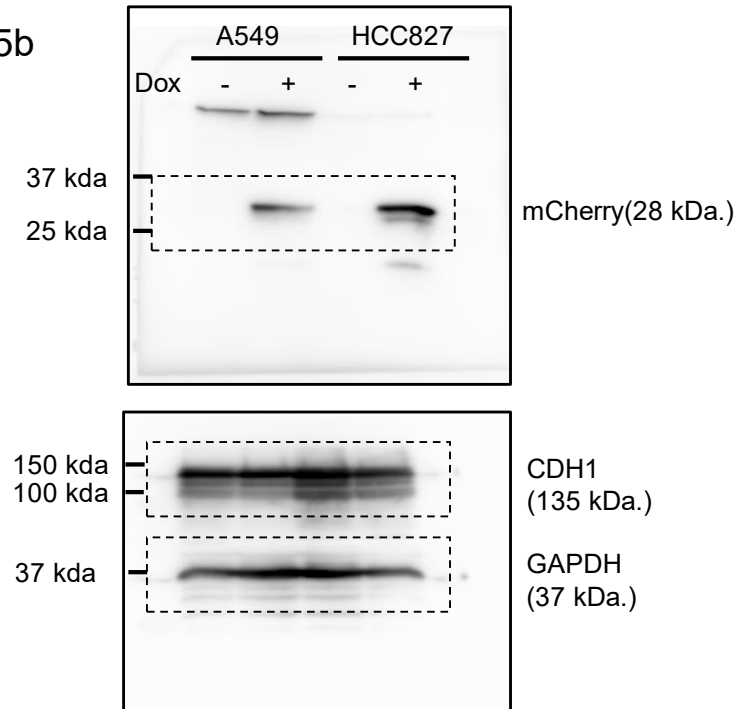


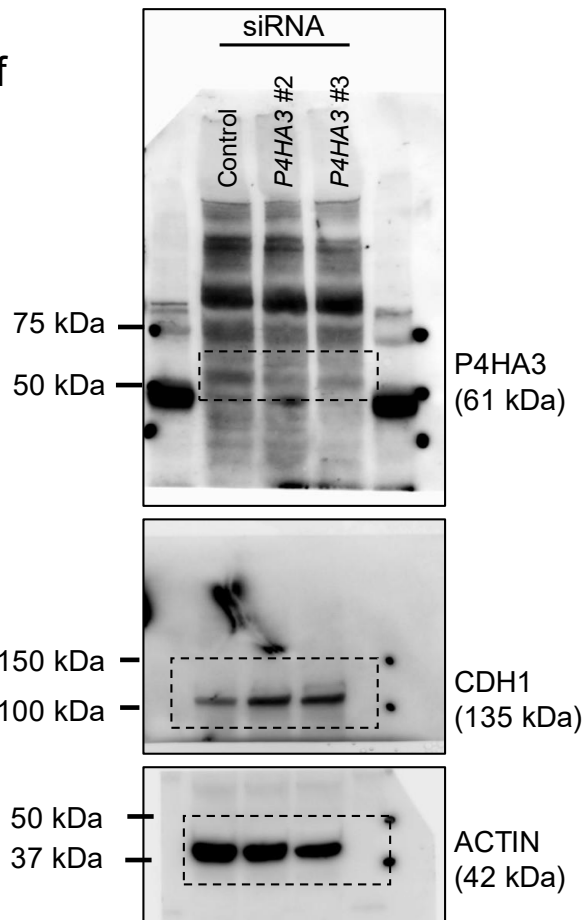
Fig. 4d



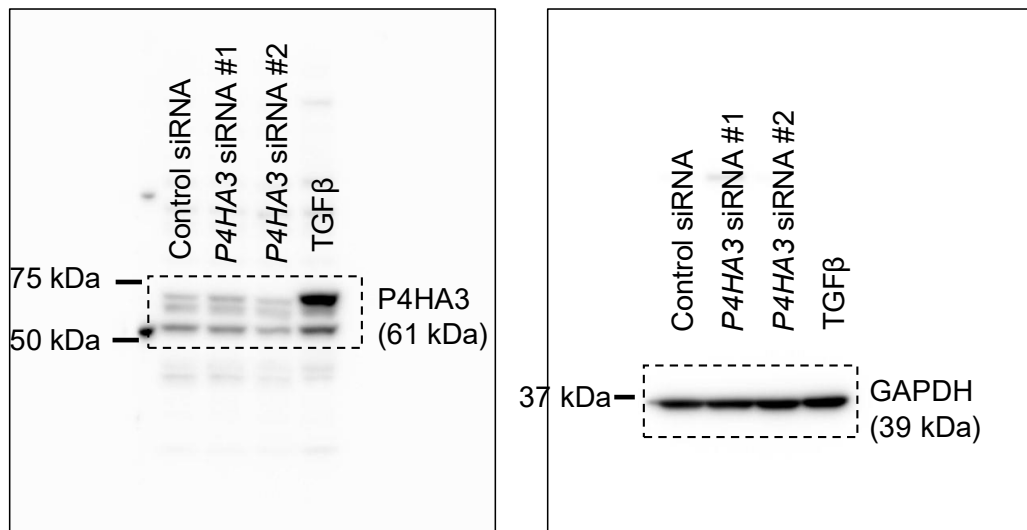
Supplementary Fig. 5b



Supplementary Fig. 5f



Supplementary Fig. 6h



Supplementary Fig. 8 Uncropped images of western blots represented in Figs. 3b, 3d, 4d, and Supplementary Figs. 3a, 3d, 5b, 5f, 6h.